La Metallurgia Italiana
International Journal of the Italian Association for Metallurgy

Heat-treatment analysis considering transformation plasticity and creep deformation for large forged steel

Y. Yanagisawa, Y. Kishi, M. Minamiya, K. Saitoh

The long cooling time during heat-treatment of a large forging due to mass effect causes creep deformation even in the transformation temperature range as well as at much higher temperatures. Therefore, the transformation plasticity and creep deformation occur simultaneously with the phase
transformation, significantly affecting the stress distribution of the forging after the heat-treatment. In this study, a FEM model factoring in the transformation plasticity and creep deformation was developed. The transformation plasticity and creep properties were measured experimentally. The proposed model was integrated into commercial FEM software ANSYS via user subroutines. The actual residual stress of the large, forged shaft was measured to compare with those of the simulations, showing that the residual stresses were mainly caused by the phase transformation stress. In particular, the transformation plastic strain and the creep strain were found to play important roles in simulating the residual stress during heat treatment of a large, forged shaft.

KEYWORDS: HEAT TREATMENT, RESIDUAL STRESS, PHASE TRANSFORMATION, TRANSFORMATION PLASTICITY, CREEP

INTRODUCTION

During heat treatments of steel objects, both thermal stress and transformation stress occur due to the temperature gradient inside the object. Special care should be paid to the heat treatment to avoid cracking and deformation caused by transient and residual stresses. Therefore, it is important for a computer simulation to estimate both the residual stress and the deformation occurring due to the heat treatment. The coupling phenomena between the temperature, stress, and metallic structure is shown in Fig. 1 [1]. So far, numerous studies of these behaviors have been conducted, and mainly applied to the quenching process [2]. Generally, the cooling rate of a large forging decreases due to the mass effect and air cooling and furnace cooling require several days. In these cases, the phase transformation stress affects the residual stress more than the thermal stress. In particular, the transformation plasticity greatly influences the stress distribution. The transformation plastic strain is a large plastic strain induced during phase transformation even under a small stress. In addition, the

Yusuke Yanagisawa, Yasuhiro Kishi
The Japan Steel Works, LTD. Muroran-shi, Hokkaido, Japan

Masahiro Minamiya, Kazuma Saitoh
Japan Steel Works M&E, Inc. Muroran-shi, Hokkaido, Japan

creep behavior, which affects the stress distribution, may occur even in the transformation temperature range as well as at much higher temperatures.

In this study, a FEM (Finite Element Method) model considering both the transformation plasticity and creep was developed. The proposed model was integrated into commercial FEM software ANSYS via user subroutines. The material properties of the transformation plasticity and creep were also measured experimentally. For experimental verification, the residual stress measurements of a large forged shaft are compared with those of the simulations.

NUMERICAL MODELING

Constitutive Equation

In this analysis, the following constitutive equations are defined based on the theory of plasticity [3]. The total strain can be divided into six parts and expressed in incremental form as Eq. [1]. Each strain increment is calculated using Eqs. [2] to [6]. The transformation plastic strain can be expressed by Eq. [5], which is reviewed by Denis [4], and the creep strain is calculated using Norton's law.

$$\Delta\boldsymbol{\varepsilon} = \Delta\boldsymbol{\varepsilon}^{e} + \Delta\boldsymbol{\varepsilon}^{p} + \Delta\boldsymbol{\varepsilon}^{th} + \Delta\boldsymbol{\varepsilon}^{m} + \Delta\boldsymbol{\varepsilon}^{tp} + \Delta\boldsymbol{\varepsilon}^{c} \quad [1]$$

$$\Delta\boldsymbol{\varepsilon}^{p} = \Delta\lambda \frac{\partial F}{\partial \boldsymbol{\sigma}} \quad [2]$$

$$\Delta\boldsymbol{\varepsilon}^{th} = \alpha \Delta T \cdot \mathbf{I} \quad [3]$$

$$\Delta\boldsymbol{\varepsilon}^{m} = \beta \Delta\xi \cdot \mathbf{I} \quad [4]$$

$$\Delta\boldsymbol{\varepsilon}^{tp} = 3K\left(1 - \xi\right)\Delta\xi\mathbf{s} \quad [5]$$

$$\Delta\boldsymbol{\varepsilon}^{c} = \frac{3}{2} A \bar{\sigma}^{n-1} \Delta t \mathbf{s} \quad [6]$$

Where $\Delta\boldsymbol{\varepsilon}^{e}$, $\Delta\boldsymbol{\varepsilon}^{p}$, $\Delta\boldsymbol{\varepsilon}^{th}$, $\Delta\boldsymbol{\varepsilon}^{m}$, $\Delta\boldsymbol{\varepsilon}^{tp}$ and $\Delta\boldsymbol{\varepsilon}^{c}$ are the tensor increments of elastic strain, plastic strain, thermal strain, phase transformation strain, transformation plastic strain, and creep strain, respectively. $\Delta\lambda$ is the plastic multiplier, F the yield function, α the thermal expansion coefficient, β the transformation dilatation, K the transformation plasticity parameter, ξ the volume fraction of the new phase, A and n the creep parameters, and s the deviatoric stress tensor, respectively.

Calculation Flow

Fig. 2 shows the calculation flow chart of the subroutine program USERMAT in ANSYS. It is assumed that all plastic strains due to the forging process itself have relaxed and thus it is stress free. At the beginning of the analysis, the phase fraction is defined. Then, the thermal strain and phase transformation strain are calculated considering the phase fraction. After the yield criterion, the implicit integration analysis, including both the transformation plastic and creep strains, is performed with the return mapping algorithm, and the equivalent stress and the equivalent plastic strain increment are updated. Finally, the consistent tangent modulus is defined. This solution procedure is repeated at each time increment.

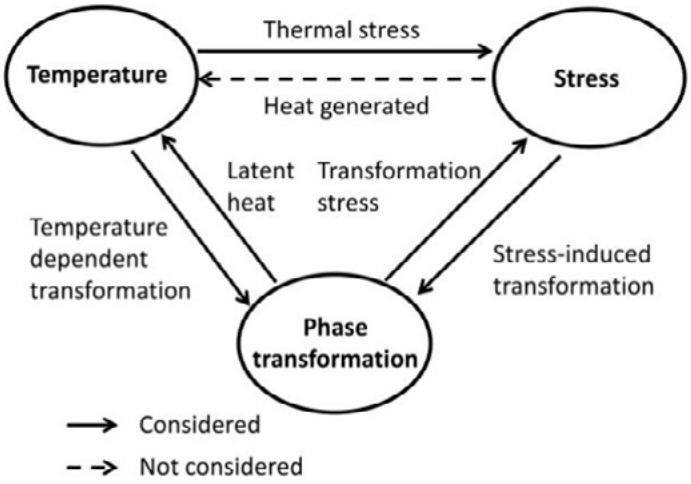

Fig.1 - Coupling model of metallo-thermo-mechanical [1]

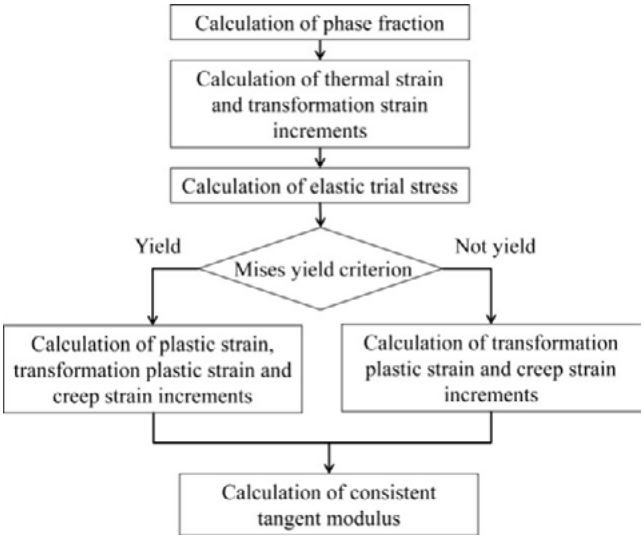

Fig.2 - The calculation flow chart.

HEAT-TREATMENT OF LARGE FORGED SHAFT

Fig. 3 shows a schematic illustration of the large forged shaft used in this study. The material was a Ni-Cr-Mo-V steel (ASTM A470M steel) used in turbine rotors. The ingot was forged using a 14,000-ton hydraulic free press. Then, the forging was heat treated at 850°C for 27 hours and air-cooled. The prior austenite grain size number of the material is about 6.0. Fig. 4 shows a comparison of the cooling curves between the experiment and the FEM analysis. The thermophysical properties such as the specific heat and the thermal conductivity were measured experimentally. The heat transfer coefficients in the calculations were estimated using the inverse analysis method, which is chosen so that the simulated temperature has the same value as the measured temperature. The cooling time to room temperature is approximately 100 hours, and the average cooling rate at the transformation temperature area was 0.17 to 0.25 °C/min. It can be presumed that the forgings had microstructures of bainite.

The residual stresses were measured in five places on the outer surface using the ring-core method. The annular groove, which has a 16 mm inner diameter, 7 mm deep, was machined around a strain gage. The residual stresses were calculated from the relaxed strains. Fig. 5 shows the residual stress measured on the outer surface. The mean axial and circumferential stresses are about 220 to 380MPa tensile stresses, re-spectively. The residual stresses of the small diameter parts (Nos. 1, 5) were equal to or higher than that of maximum diameter part (No. 3). In spite of the relatively large difference in diameter, there is no significant correlation between the diameter and the residual stress.

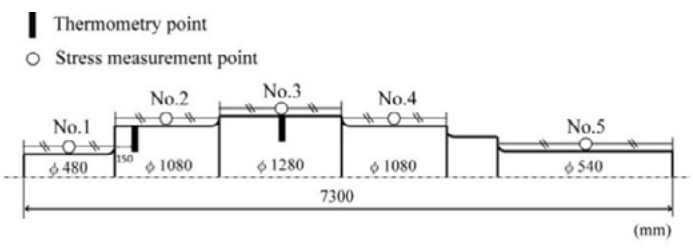

Fig.3 - Schematic illustration of large forged shaft.

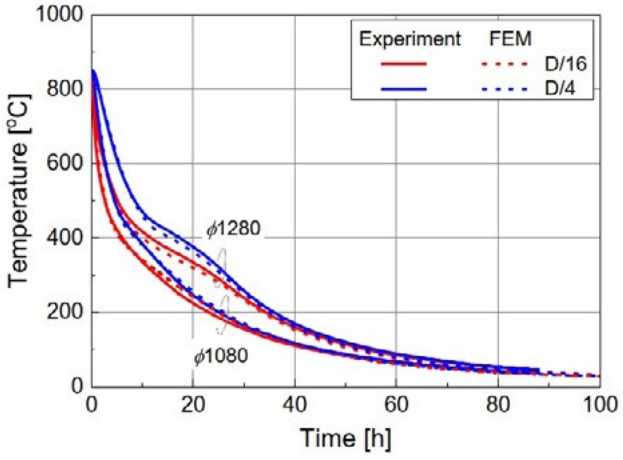

Fig.4 - Comparison of cooling curves.

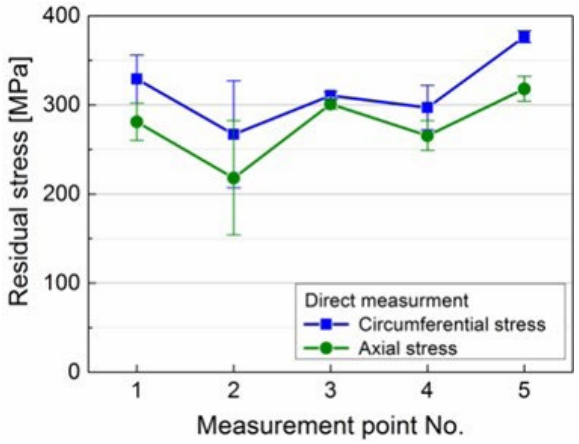

Fig.5 - Residual stress measured at the outer surface.

ANALYSIS OF RESIDUAL STRESS.

Determination of Material Parameters

The material parameters for numerical modeling are decided from the following procedures. The materials are Ni-Cr-Mo-V steel (ASTM A470M steel). The literature values were used for elastic modulus and Poisson's ratio. The linear expansion coefficient and transformation strain were determined from thermal expansion tests, and the stress-strain curves were measured from tensile tests at various temperatures. The parameters of multi-phases (austenite and bainite) are calculated according to the linear mixture rule for the phase mixture. The Johnson-Mehl-Avrami-Kolmogorov equation is used to depict the transformation kinetics of the bainitic transformation. Fig. 6 shows a comparison between the measured and the calculated phase fractions. In the cooling rate range from 0.1 to 0.5°C/min, the calculated volume fraction corresponds to the measured one.

The transformation plasticity tests were performed using a hot-working simulator (Fuji Electronic Industrial, Thermec Mastor_Z) and round-bar specimens with a diameter of 8mm. The specimens were heated to 850°C and cooled rapidly to 450°C, and a stress was applied at 450°C and maintained at a constant level. The cooling rate was 2°C/min during phase formation. The round-bar specimens were measured perpendicular to their axes using a continuous laser sensor during cooling. Fig. 7 shows the relation between the temperature and the total diametral strain during cooling. When the axial stresses were applied, the bainite transformation strain in the direction of the diameter decreased. This indicates that there was transformation plasticity. The transformation plastic strain can be calculated as the deviation between the stress-free total strain value and the strain value with a small applied stress. As shown in Fig. 8, linear relationships are seen between the applied stress and the transformation plastic strain under tensile or compressive stresses. The obtained results give $9.5 \cdot 10^{-5}$ MPa^{-1} for the value of K under the tensile stress, and $12.2 \cdot 10^{-5}$ MPa^{-1} under the compressive stress. Because the difference in the values of K under tensile and compressive stress is small, the value of K under the tensile stress was used in this analysis.

The creep parameters were determined from a creep database of SUS304 steel [5] for the austenite phase, and from the results of the stress relaxation test for the bainite phase. Fig. 9 show the relationship between stress and creep strain rate of the bainite phase. The stress relaxation behavior is different between the high stress and the low stress regions at temperatures of 250 and 300°C, in contrast to the results at temperatures from 350 to 500°C. This is because about 5% austenite is inevitably retained in the specimen, and the stress relaxations occur due to both the retained austenite transformation and the creep deformation from 250 to 300°C. These stress-relaxation behaviors are expressed by a creep constitutive equation using Norton's law, which can well explain the creep behavior under the low stress as shown in Fig. 9.

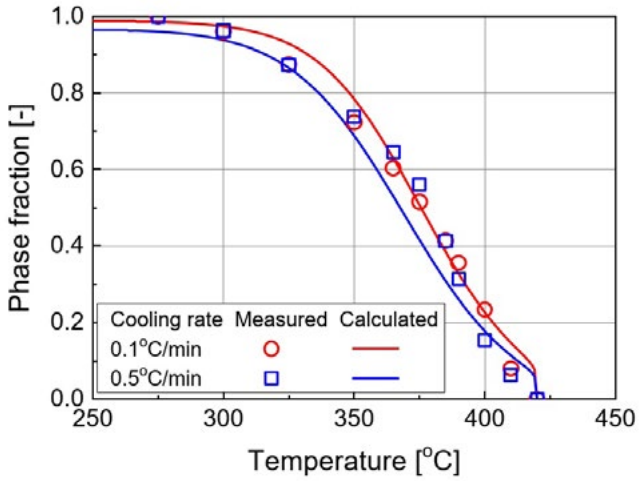

Fig.6 - Measured and calculated phase fraction.

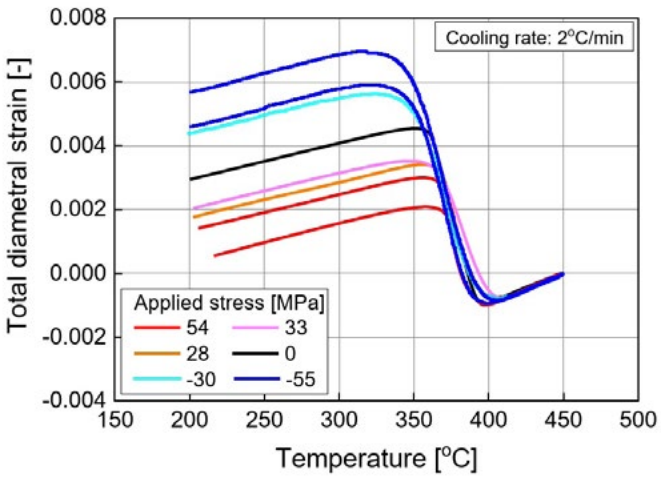

Fig.7 - Temperature-strain diagrams.

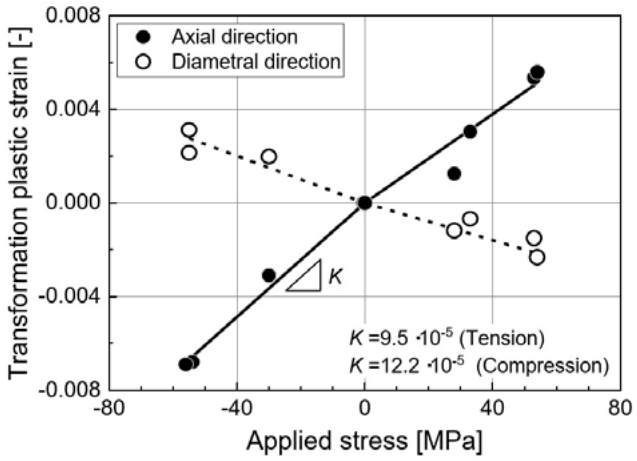

Fig.8 - Transformation plastic strain.

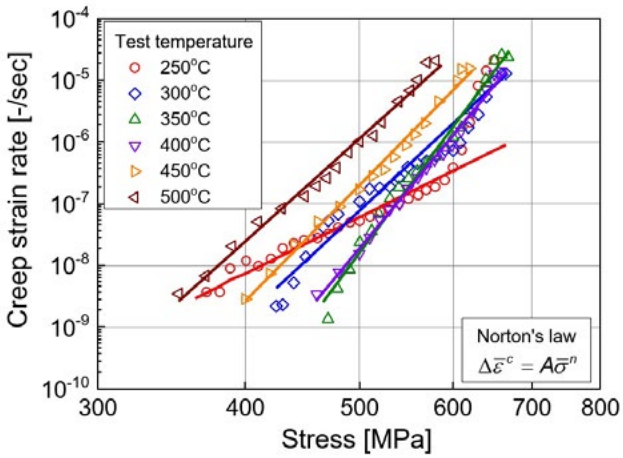

Fig.9 - Creep strain rate of the bainite phase.

Verification of Residual Stress Calculation

In order to clarify the relative effects of the transformation plasticity and creep, three analysis conditions were chosen: (a) eliminating the transformation plastic strain and creep strain in Eq. [1], (b) considering only the transformation plastic strain, and (c) considering both strains. The stresses analyzed are shown in Fig. 10 and Fig. 11. There is a little residual stress without the transformation plasticity, and the difference is on the dangerous side in terms of cracking at the surface. The simulated residual stresses are tension when the transformation plasticity is considered, but the tensile stress analyzed was higher than the measurements from the large diameter parts. The analyzed surface stresses tend to approach the measured stresses when the stress relaxation is considered. The effect of stress relaxation at the surface of large diameter parts was higher than that at the surface of the small parts, because the surface stresses increase with increasing diameter. As shown in the above, both the transformation plastic strain and the creep strain play important roles in simulating the residual stress in the heat treatment of a large forged shaft.

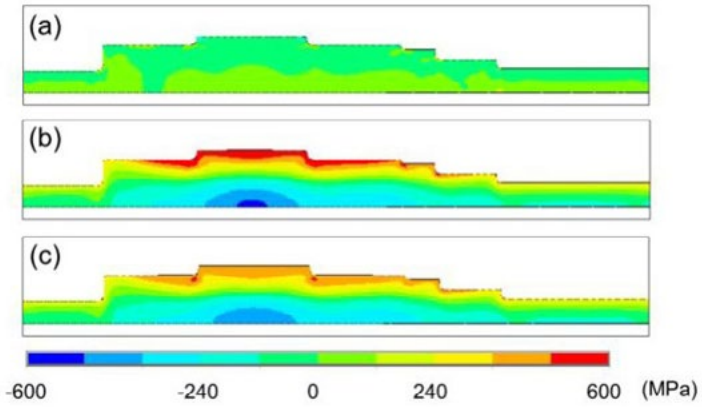

Fig.10 - Distribution of the circumferential residual stress.

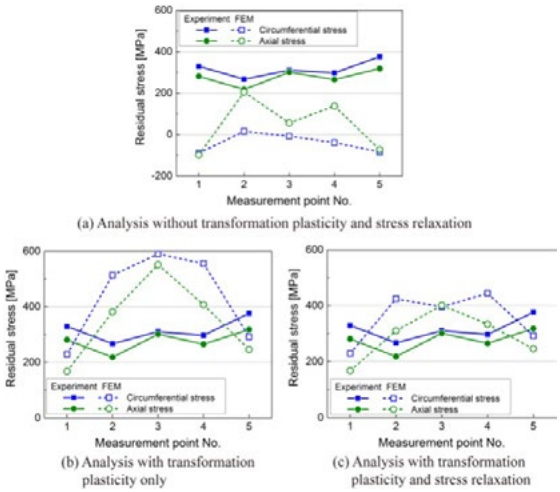

Fig.11 - Comparison of residual stress.

CONCLUSIONS

A FEM model considering both the transformation plasticity and creep deformation was developed to predict the residual stresses of a large forged shaft. The validity of the calculation was verified by comparing the residual experimental and analytical stresses. From the results, the following conclusions are obtained:

1) The experimental mean surface stresses of the large forged shaft were about 220 to 380 MPa in tension, showing that the residual stresses were mainly caused by the transformation stress.

2) No residual stresses are found to be generated without transformation plasticity, while the simulated residual stress considering the transformation plasticity has the same tendency as the experimental one.

3) The analyzed surface stresses tend to approach the measured stresses when the stress relaxation is considered.

ACKNOWLEDGEMENT

This paper is reproduced from the authors' previous work [Y. Yanagisawa, Y. Kishi, and K. Sasaki, "Analysis of Residual Stresses During Heat Treatment of Large Forged Shafts Considering Transformation Plasticity and Creep Deformation", Strength of Materials, 49, No. 2, 239-249 (2017)] with permission from Springer Nature.

REFERENCES

[1] T. Inoue and Z. Wang. Coupling between stress-temperature-metallic structures during processes involving phase-transformations, Mater. Sci. Technol, 1, No. 10, 845-850 (1985).
[2] M. Fukumoto, M. Yoshizaki, H. Imataka, K. Okamura and K. Yamamoto. Three-dimensional FEM analysis of helical gear subjected to the carburized quenching process, J. Soc. Mater. Sci., Jpn., 50, No. 6, 598-605 (2001).
[3] E. A. de Souza Neto, D. Peric and D. R. J. Owen, Computational methods for plasticity, Wiley & Sons, (2008), Kenjiro Terada (Supervised translation).
[4] S. Denis, E. Gautier, A. Simon and G. Beck. Stress phase-transformation interactions-basic principles, modeling, and calculation of internal-stresses, Mater. Sci. Technol, 1, No. 10, 805-814 (1985).
[5] National research institute for metals, NRIM Creep data sheet No. 4B, 1986.

TORNA ALL'INDICE >